

## THE COMBINED EFFECT OF NANOFUID AND REFLECTIVE MIRRORS ON THE PERFORMANCE OF PHOTOVOLTAIC/THERMAL SOLAR COLLECTOR

by

**Omer Khalil AHMED<sup>a\*</sup> and Shaimaa Mohammed BAWA<sup>b</sup>**

<sup>a</sup>Technical Institute-Hawija, Northern Technical University, Kirkuk, Iraq

<sup>b</sup>Technical College-Kirkuk, Northern Technical University, Kirkuk, Iraq

Original scientific paper

<https://doi.org/10.2298/TSCI171203092A>

*A photovoltaic/thermal solar collector is a system which is capable of producing both electricity and thermal energy. However, this technology still needs more studies. In this paper, a mathematical model was presented to study the performance of a photovoltaic/thermal collector by using the upper and lower reflectors with the presence of glass cover. Water and nanofluids ( $Al_2O_3-H_2O$ ) were used as cooling medium. A computer program was proposed to calculate the amount of solar radiation reflected on the reflected mirrors and then absorbed by the hybrid collector and study the effect of nanofluid on the performance of the system.*

*Solar radiation absorbed by the collector can be increased using the upper and lower reflectors to  $1138 W/m^2$  while it can reach  $950 W/m^2$  with the upper reflector and  $746 W/m^2$  with the lower reflector. It was noticed that when using reflective mirrors, the outlet water temperature increased by 21.7%. Meanwhile, the outlet water temperature increased by 0.44% when nanofluid was used as a cooling medium. The average of daily thermal efficiency as a result of using two reflectors without nanofluid was 62.1%, while the thermal efficiency was 59.735% without using any reflector, meaning a positive effect of using reflectors on the thermal efficiency. The electrical efficiency reduced with the existence of the reflective mirrors, whereas the daily average of the total electrical efficiency without the reflective mirror and using the nanofluid was (14.6%), while with a reflective mirror and using nanofluid, the daily average was (13.67%).*

Key words: *photovoltaic/thermal collector; nanofluid, reflective mirrors, performance*

### Introduction

The use of solar energy to generate electricity is one of the most important applications at the present time as these cells convert solar energy into a constant current [1]. However, the disadvantage of these cells is the high temperature during work, especially in hot sunny climates as in the Middle East which is characterized by a hot climate for most days of the year. The high temperature of cells causes a decrease in their efficiency. For this reason, researchers have tried to improve the performance of solar cells by withdrawing the heat generated in them and making use of them for heating and other industrial purposes [2]. Hybrid solar collectors, photovoltaic/thermal (PV/T) collector supply electricity and hot water or hot air at the same

\* Corresponding author, e-mail: omerkalil@yahoo.com

time. They integrate the two systems together: solar cells and heaters [3]. This system is mainly designed to increase the electrical efficiency of solar cells by drawing heat from these cells.

Kostić *et al.* [3, 4] studied the effect of using aluminum mirrors on the performance of hybrid solar collectors. The produced thermal and electrical energies increased considerably when using the reflectors in an ideal method with the ideal angle calculated to be  $66^\circ$ . Tabet *et al.* [5] studied the effect of using a plane reflector to improve the performance of PV/T air collector in Algeria. A mathematical model was presented to show the effect of the reflector. The study showed that there was an improvement in the performance of the collector when using this reflector.

Naik and Palatel [6] used a single mirror mounted on the top of the hybrid solar collector and at angles ranging from  $85-100^\circ$  in the Indian city of Kolkata, which enjoys a tropical climate. Baccoli *et al.* [7] analyzed the mathematical model of a flat solar collector connected to an external inverter at the bottom edge of the collector. The mathematical model was developed and used to estimate the solar radiation passing through a transparent cover of the collector with and without a reflector. Bahaidarah *et al.* [8] presented an experimental and analytical study of the effect of the mirrors placed at an angle on the performance of a hybrid solar collector. Belhadj [9] studied the effect of the angle of two reflective plates to increase the intensity of solar radiation on solar cells. Chowdhury [10] analyzed a concentrated hybrid PV/T collector. The goal of this design was to increase the total efficiency of the hybrid collector. The overall efficiency of the collector was about 80%. Rosli *et al.* [11] studied the thermal efficiency of a polymer collector with unglazed PV/T system. The thermal efficiency of the system was 47%. Soltani *et al.* [12] improved the photovoltaic efficiency of the PV/T collector by using the nanofluid technique. Five different cooling methods were used practically, namely natural convection, forced air cooling, water cooling,  $\text{SiO}_2$ -water nanofluid cooling, and  $\text{Fe}_3\text{O}_4$ -water nanofluid cooling. The results indicated that the water nanofluid cooling by using  $\text{SiO}_2$  materials, which were found to have the highest power and optimum efficiency, showed 54.29% and 3.35% improvement, respectively, compared to the natural cooling method.

A mathematical model was performed by Mustafa *et al.* [13] to evaluate the performance of PV/T nanofluid system. The goal of this article is to study theoretically a new design of the PV/T system which includes stainless steel rectangular tube. Nanofluid provides a higher performance, where the electrical and thermal efficiencies of this system obtained approximately 14.38% and 71.71% at the mass-flow rate of 0.174 kg/s and  $650 \text{ W/m}^2$  solar radiation. Colangelo *et al.* [14] presented a new design of PV/T collector, this new design of hybrid system was analyzed using commercial software for thermal simulations, two models have been investigated: vertical configuration and horizontal configuration, considering a flow rate of 0.1 L per minute and of 0.5 L per minute of fluid, with a tilt of  $30^\circ$ . An analytical study has been carried out by Tripathi *et al.* [15] to study the performance of three cases for PV/T collector at constant flow rate. This study showed that the N-convectional compound parabolic concentrator collector connected in series is chosen superior than other cases.

Hussein *et al.* [16] utilized the nanoparticle type (Zn-water) to improve the performance of the hybrid PV/T collector. The results showed that using the nanofluid led to improved electrical and thermal efficiency of the collector. Ghadiri *et al.* [17] the effects of ferrofluids as a coolant on the overall efficiency of a PV/T, PV/T unit used nanofluid type ( $\text{Fe}_3\text{O}_4$ -water) with concentrations ranging from 1-3% to improve the performance of the hybrid solar collector and found an increase in the efficiency of the hybrid collector (3%). Kim *et al.* [18] studied the effect of using glass cover on the performance of the hybrid solar collector used to heat the water and found that it improved thermal efficiency by 14% while the electrical efficiency de-

creased by 1.4%. Glass is an undesirable option when the priority is to produce electric power. Al-Shamani *et al.* [19] used nanofluid such as TiO<sub>2</sub>-water, SiO<sub>2</sub>-water, and SiC-water as a coolant in the PV/T collector that contains serpentine shaped absorber design with rectangular cross-section. The results showed that the PV/T collector with SiC nanofluid had the highest combined thermal performance of 81.73% and electrical efficiency of 13.52%. Sardarabadi *et al.* [20] studied the effect of using metal-oxides-water as nanofluids in the PV/T collector. This study showed that the overall exergy efficiencies for the cases of PV/T-water, PV/T-TiO<sub>2</sub>, PV/T-Al<sub>2</sub>O<sub>3</sub>, and PV/T-ZnO are enhanced by 12.34%, 15.93%, 18.27%, and 15.45%, respectively, compared to that of the solar cell with no collector. Potenza *et al.* [21] studied the performance of parabolic trough collector, with transparent receiver tube, based on gas-phase nanofluid. Two coaxial tubes, with vacuum in the inner space were used as receiver pipe. Colangelo *et al.* [22] used numerical software to investigate the effect of nanofluid on the performance of the solar thermal collector. The study showed that there was an improvement in the performance of the collector when using the nanotechnology. The researchers found that when using nanofluid, an increase in the thermal efficiency of the system has been achieved by (7.45%). Chemisana *et al.* [23] using a Fresnel lens to enhance the performance of the PV/T collector for building – façade integration. This study showed that the electric power generated by this system is about 4.5-4.7 time higher than in the classical PV/T collector. Also, the thermal power ratio takes a value ranging from 1.9 to 2.8 depending on the weather conditions.

By reviewing the literature related to the study of the performance of PV/T solar collectors, no study was found combining the effects of reflective mirrors and nanofluid on the performance of these systems. Therefore, this study will focus on the study of variables affecting the performance of the systems with reflective mirrors and nanofluid to achieve a clear understanding of their effects and improve the performance of the hybrid PV/T collector.

### Mathematical models

The design of the hybrid solar collector used in this study consists of one glass cover, the solar cell, heat exchanger coated with the aluminum sheets on the back side of the solar cell, upper reflector connected to the upper side of the hybrid collector and the lower reflector connected to the lower side of the hybrid collector. The PV/T collector with the reflective mirrors system is shown in fig. 1. The collector type is serpentine as shown in fig. 2.

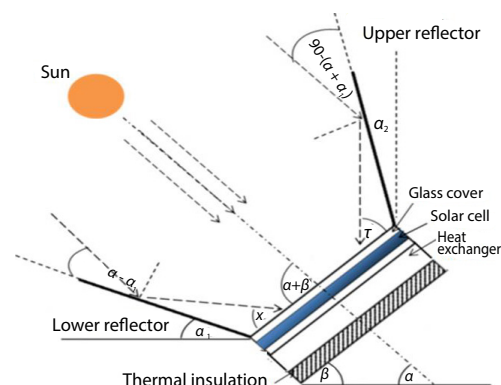


Figure 1. Schematic diagram of the PV/T collector

### Solar radiation calculations

The isotropic diffuse model was used to estimate the rate of solar radiation [11]. The total radiation,  $S_{total}$ , on the tilted PV/T collector included five components: the direct radiation,  $I_b$ , diffuse radiation,  $I_d$ , solar radiation reflected from the ground,  $I_g$ , radiation reflected,  $I_{up-ref}$ , from upper reflector to the surface of PV panel with tilted plane angle,  $\alpha_1$ , and the radiation reflected,  $I_{lo-ref}$ , from the bottom mirror to the solar cell with tilted plane angle,  $\alpha_2$ , as shown in fig. 1. Therefore the total absorbed solar radiation on the tilted surface is the sum of five terms as:

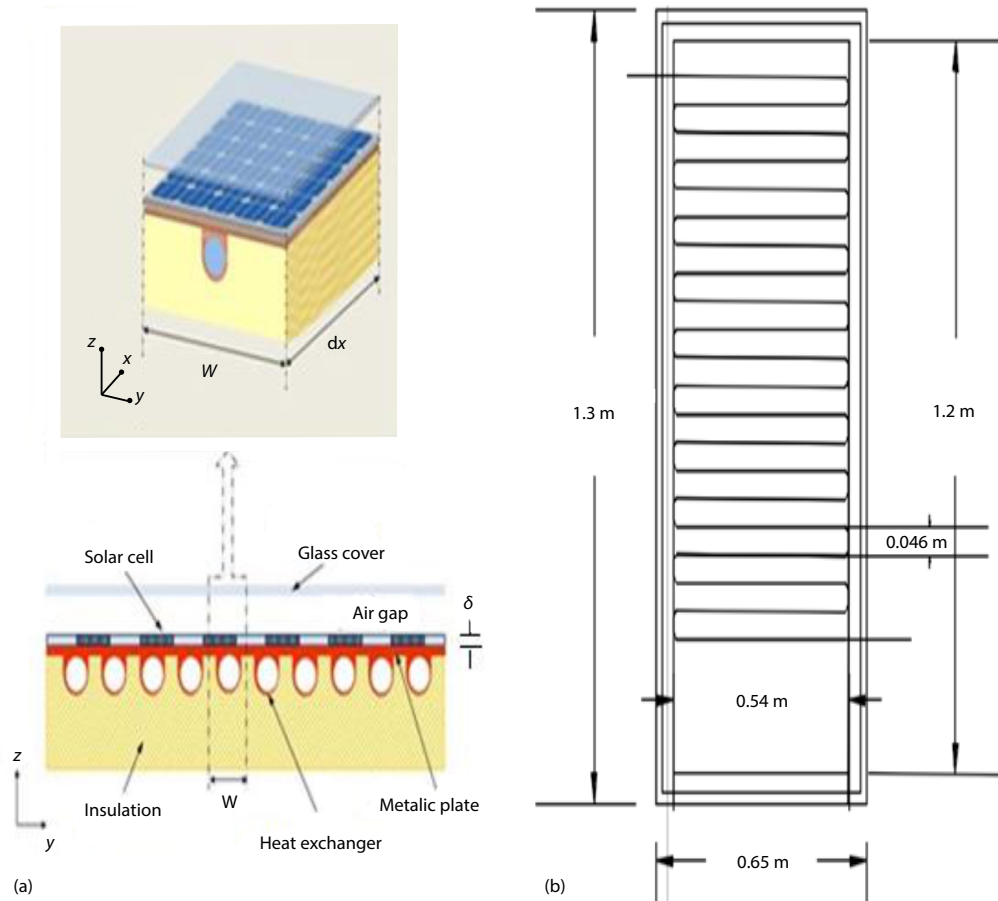


Figure 2. Sketch and structures of the experimental set-up of the hybrid PV/T collector; (a) structure of heat exchanger, (b) the dimensions of the heat exchanger

$$S_{\text{total}} = I_b + I_d + I_g + I_{\text{up-ref}} + I_{\text{lo-ref}} \quad (1)$$

The radiation components are calculated from the following equations [24]:

$$I_b = I_{\text{total}} \sin(\alpha + \beta) (\tau\alpha)_b \quad (2)$$

$$I_d = I_{\text{diffuse}} \left( \frac{1 + \cos\beta}{2} \right) (\tau\alpha)_d \quad (3)$$

$$I_g = \rho_g I_{\text{total}} \left( \frac{1 - \cos\beta}{2} \right) (\tau\alpha)_g \quad (4)$$

where  $\rho_g$  is the ground reflectance ( $= 0.4$ ) [25]. The reflected radiation from upper reflector,  $I_{\text{up-ref}}$ , with tilted mirror angle,  $\alpha_1$ , and reflected radiation from lower reflector,  $I_{\text{lo-ref}}$ , with tilted mirror angle,  $\alpha_2$ , are defined:

$$I_{\text{up-ref}} = \rho_{A_1} I_{\text{total}} \sin(\tau) \sin(\alpha + \alpha_1) (\tau\alpha)_b, \quad \tau = \alpha + 2\alpha_1 - \beta \quad (5)$$

$$I_{\text{lo-ref}} = \rho_{A_1} I_{\text{total}} \sin(x) \sin(\alpha - \alpha_2) (\tau\alpha)_b, \quad x = \beta + 2\alpha_2 - \alpha \quad (6)$$

The angles  $x$  and  $\tau$  are explained in fig. 1. The total solar radiation,  $I_{\text{total}}$ , diffused radiation,  $I_{\text{diffuse}}$ , solar altitude angle,  $\alpha$ , and transmittance-absorptance product,  $\tau\alpha$ , were calculated according to the procedure as discussed in [24].

*Thermophysical properties of nanofluid (Al<sub>2</sub>O<sub>3</sub>-water)*

Pure water is selected as the base-fluid with temperature dependent properties as shown in tab. 1 [25]. The Al<sub>2</sub>O<sub>3</sub> was used as nanoparticles in this study, the properties of Al<sub>2</sub>O<sub>3</sub> used for the modelling are summarized from references [26]. Thermophysical properties of the working fluid (Al<sub>2</sub>O<sub>3</sub>-water nanofluid) are changed due to influence of the nanoparticles. These properties can be found from standard tables or equations.

**Table 1. Variation of water properties with the temperature**

Density [kgm <sup>-3</sup> ]	$\rho_w = 1000 - 0.0178 [T-277]^{1.7}$
Viscosity [kgm <sup>-1</sup> s <sup>-1</sup> ]	$\mu_w = 1.788 \cdot 10^{-3} \exp [-1.704 - (1448.5 / T) + (521926.58 / T^2)]$
Thermal conductivity [Wm <sup>-1</sup> K <sup>-1</sup> ]	$K_w = -8.01 \cdot 10^{-6} (T - 273)^2 + 1.94 \cdot 10^{-3}(T - 273) + 0.536$
Specific heat [Jkg <sup>-1</sup> K <sup>-1</sup> ]	$c_w = 4.1855 \cdot 10^3 [0.966185 + 0.0002874 ((T - 173) / 100)^{5.26}]$

The properties of nanofluids can be estimated by using the following equations:

$$\rho_{\text{eff}} = \rho_w (1 - \phi) + \rho_n \phi \tag{7}$$

where  $\rho_{\text{eff}}$  is the nanofluid density,  $\rho_w$  and  $\rho_n$  are the water and Al<sub>2</sub>O<sub>3</sub> densities.

The  $\phi$  is the nanofluid volume fraction calculated as [27]:

$$\phi = \frac{\frac{m_n}{\rho_n}}{\frac{m_n}{\rho_n} + \frac{m_w}{\rho_w}} \tag{8}$$

where  $m_n$  and  $m_w$  are the mass of Al<sub>2</sub>O<sub>3</sub> and water, respectively.

The heat capacity of nanofluid ( $C_{\text{eff}}$ ) is calculated from [22]:

$$C_{\text{eff}} = \frac{\phi \rho_n c_n + (1 - \phi) \rho_w c_w}{\rho_{\text{eff}}} \tag{9}$$

where the  $c_n$  and  $c_w$  are the heat capacity of Al<sub>2</sub>O<sub>3</sub> and water, respectively.

The viscosity of nanofluid is given by [16]:

$$\mu_{\text{eff}} = \frac{\mu_w}{(1 - \phi)^{2.5}} \tag{10}$$

The Maxwell equation is used to evaluate the thermal conductivity of nanofluid,  $K_{\text{eff}}$ , as [26]:

$$K_{\text{eff}} = \frac{K_n + 2K_w + 2\phi(K_n - K_w)}{K_n + 2K_w - \phi(K_n - K_w)} K_w \tag{11}$$

where the  $K_n$  and  $K_w$  are the thermal conductivity of Al<sub>2</sub>O<sub>3</sub> and water, respectively.

The Prandtl number can be calculated from the following equation [28]:

$$\text{Pr}_{\text{eff}} = \frac{\mu_{\text{eff}} C_{\text{eff}}}{K_{\text{eff}}} \tag{12}$$

*Thermal modeling of the system*

To model the PV/T collector, a number of simplified assumptions are as follows [24]:

- the flow in the system is incompressible, laminar, and uniform,
- performance is a semi steady-state,
- heat flow through a cover is 1-D and temperature drop through a cover was negligible; also, there is 1-D heat flow through back insulation,
- the sky can be considered as a blackbody for long-wavelength radiation at an equivalent sky temperature,
- temperature gradients around tubes can be neglected; the temperature gradients in the direction of flow and between the tubes can be treated independently,
- loss through front and back are to the same ambient temperature,
- dust and dirt on the collector are negligible,
- shading of the collector absorber plate is negligible, and
- nanofluid is assumed as a single phase fluid.

Mainly, the energy input to the PV/T solar collector is in the form of solar radiation from the Sun and the thermal fluid flowing inside the heat exchanger from the inlet. The energy from the system is due to the heat loss by convection and thermal fluid outflow from the collector. The total thermal energy gain by PV/T collector is expressed as [29]:

$$\bar{Q}_u = A_c \bar{F}_R [\bar{S} - \bar{U}_{loss} (T_{f.in} - T_a)] \quad (13)$$

where  $\bar{F}_R$  is called the modified collector heat removal factor and calculated for the serpentine arrangement of PV/T collector from the following equation [24]:

$$\bar{F}_R = F_1 F_3 F_5 \left[ \frac{2F_4}{F_6 \exp \left[ -\sqrt{1 - F_2^2 / F_3} \right] + F_5} - 1 \right] \quad (14)$$

$$F_1 = \frac{\kappa}{U_{loss} W} \frac{\kappa R(1 + \gamma)^2 - 1 - \gamma - \kappa R}{[\kappa R(1 + \gamma) - 1]^2 - (\kappa R)^2}, \quad F_2 = \frac{1}{\kappa R(1 + \gamma)^2 - 1 - \gamma - \kappa R}, \quad F_3 = \frac{\dot{m} C_p}{F_1 U_L A_c}$$

where

$$F_4 = \left( \frac{1 - F_2^2}{F_2^2} \right)^{0.5}, \quad F_5 = \frac{1}{F_2} + F_4 - 1, \quad F_6 = 1 - \frac{1}{F_2} + F_4$$

$$\kappa = \frac{(K \delta U_{loss})^{1/2}}{\sinh \left[ (W - D)(U_{loss} / K \delta)^{1/2} \right]}, \quad \gamma = -2 \cosh \left[ (W - D) \left( \frac{U_{loss}}{K \delta} \right)^{1/2} \right] - \frac{D U_L}{\kappa}, \quad R = \frac{1}{C_b} + \frac{1}{\pi D h_{fi}}$$

where  $\delta$ , fig. 2(a), is the thickness of the solar cell,  $c_p$  – the specific heat of nanofluid,  $K$  – the thermal conductivity of the material,  $U_L$  – the overall heat loss coefficient of a collector, and  $h_{fi}$  – the convection heat transfer coefficient inside the tube and calculated for the nanofluid from the following relations [16]:

$$h_{f,i} = \frac{K_{eff}}{D} \left[ 4.36 + \frac{0.086 \left( \frac{Re_{eff} Pr_{eff} D}{L} \right)^{1.33}}{1 + Pr_{eff} \left( \frac{Re_{eff} D}{L} \right)^{0.83}} \right], \quad Re_{eff} = \frac{4\dot{m}}{\pi D \mu_{eff}}$$

where  $W$  is the distance between the tubes,  $D$  – the tube diameter,  $C_b$  – the bond conductance, and  $L$  – the length of the tube.

The portion of solar radiation incident on the solar cell is converted into electricity, therefore the modified solar radiation can be calculated from the following equation [30]:

$$\bar{S} = S_{\text{total}} \left[ 1 - \frac{\eta_{\text{PV}}}{\alpha_{\text{PV}}} \right] \quad (15)$$

where  $\eta_{\text{PV}}$  is the instantaneous electrical efficiency of the PV cells at their operating temperature and it be calculated from the following equation [31]:

$$\eta_{\text{PV}} = \eta_{\text{ref}} [1 - B(T_{\text{PV}} - T_{\text{ref}})] \quad (16)$$

where  $\eta_{\text{ref}}$  is the standard cell efficiency at reference temperature ( $T_{\text{ref}} = 25$  °C).

The modification heat loss coefficient can be calculated from the following equation:

$$\bar{U}_{\text{loss}} = U_{\text{loss}} - \frac{S}{\alpha_{\text{PV}}} \eta_{\text{ele}} B \quad (17)$$

The outlet temperature can be calculated from the following equation:

$$T_{\text{f,out}} = \frac{\bar{Q}_u}{\dot{m} C_{\text{eff}}} + T_{\text{fin}} \quad (18)$$

The total thermal energy gain by PV/T collector in terms of the mean solar cell temperature can be expressed as [24]:

$$\bar{Q}_u = A_c [\bar{S} - \bar{U}_{\text{loss}} (T_{\text{pv,m}} - T_a)] \quad (19)$$

The mean solar cell temperature can be solved by equating eqs. (13) and (19) to get:

$$T_{\text{pv,m}} = \frac{\bar{Q}_u}{\bar{F}_R \bar{U}_{\text{loss}}} (1 - \bar{F}_R) + T_{\text{fin}} \quad (20)$$

The heat loss coefficient,  $U_{\text{loss}}$ , is the summation of three components [32]:

$$U_{\text{loss}} = U_{\text{top}} + U_{\text{back}} + U_{\text{edge}} \quad (21)$$

The top loss coefficient is given by [33]:

$$U_t = \left( \frac{1}{h_w + h_{\text{rgs}}} \right)^{-1} \quad (22)$$

where  $h_w$  is the wind heat transfer coefficient and calculated by [24]:

$$h_w = 5.7 + 3.8V_{\infty} \quad (23)$$

where  $V_{\infty}$  [ $\text{ms}^{-1}$ ] is the wind velocity and  $h_{\text{rgs}}$  – the radiation heat transfer coefficient between the glass cover and the sky obtained as follows [14]:

$$h_{\text{rgs}} = \varepsilon_g \sigma (T_g^2 + T_s^2) (T_g + T_s) \quad (24)$$

where  $T_g$  [°C] is the mean glass temperature,  $\varepsilon_g$  – the glass emittance, and  $T_s$  – the sky temperature and calculated from the following equation [34]:

$$T_s = 0.0558.T_a^{1.5} \quad (25)$$

The heat transfer from the edges can be neglected while the back heat transfer coefficient,  $U_b$ , can be evaluated by considering conduction and convection from the bottom of the hybrid collector as:

$$U_b = \left( \frac{L_b}{k_b} + \frac{1}{h_w} \right)^{-1} \quad (26)$$

where  $L_b$  and  $k_b$ , are the thickness and thermal conductivity of the insulation (glass wool).

The electrical power can be calculated from the following equation [35]:

$$Q_{\text{ele}} = \frac{A_c S \eta_{\text{PV}}}{\alpha_{\text{PV}}} \left\{ 1 - \frac{\eta_{\text{ref}} \beta}{\eta_{\text{PV}}} \left[ \bar{F}_R (T_{\text{fin}} - T_a) + \frac{\bar{S}}{\bar{U}_{\text{loss}}} (1 - \bar{F}_R) \right] \right\} \quad (27)$$

The thermal efficiency of the system can be calculated using the following equation [36]:

$$\eta_{\text{th}} = \frac{Q_u}{I_{\text{total}} A_c} \quad (28)$$

Also, the electrical efficiency of the PV/T hybrid collector evaluated from the relation [37]:

$$\eta_{\text{ele}} = \frac{Q_{\text{ele}}}{I_{\text{total}} A_c} \quad (29)$$

The overall efficiency of the hybrid air collector is the summation of thermal and electrical efficiencies:

$$\eta_{\text{overall}} = \eta_{\text{ele}} + \eta_{\text{th}} \quad (30)$$

The MATLAB program was used to solve the above equations to obtain the theoretical results and compare these results with the experimental data.

## Results and discussions

This article presents the results of a study done to assess the combined effect of nanofluid and reflective mirrors on the performance of hybrid solar collector under Iraqi climate conditions. The system was set towards the south to benefit from a large extent of Sun radiation. The collector tilted plane angle,  $\beta$ , was  $45^\circ$ . The angle of the upper and lower reflectors was  $5^\circ$  and  $35^\circ$ , respectively. Table 2 shows weather conditions during test (March, 29) of Kirkuk city ( $35.46^\circ\text{N}$  and  $44.39^\circ\text{E}$ ) in Iraq. The system was put towards the south to benefit from a large extent of Sun radiation. The collector tilted plane angle was  $45^\circ$ .

**Table 2. The weather condition for the test day**

Time [h]	$T_{\text{ambient}} [^\circ\text{C}]$	Wind velocity [ $\text{msec}^{-1}$ ]	Solar radiation [ $\text{Wm}^{-2}$ ]
8	23.9	0.1	434.66
9	21.5	0.2	533.0
10	22.8	0.3	597.43
11	23.6	0.1	626.95
12	24.3	0.1	615.08
13	24.4	0.4	565.61
14	25.6	0.3	481.56
15	25.9	0.9	366.81
16	24.6	0.5	208.66

### Absorbed solar radiation

Figure 3 shows the variation of total absorbed solar radiation in the PV/T collector calculated from eq. (1). The value of solar radiation increased with time and reached its maximum value of 558 W/m<sup>2</sup> at 12 noon for this particular day without using any reflective mirrors.

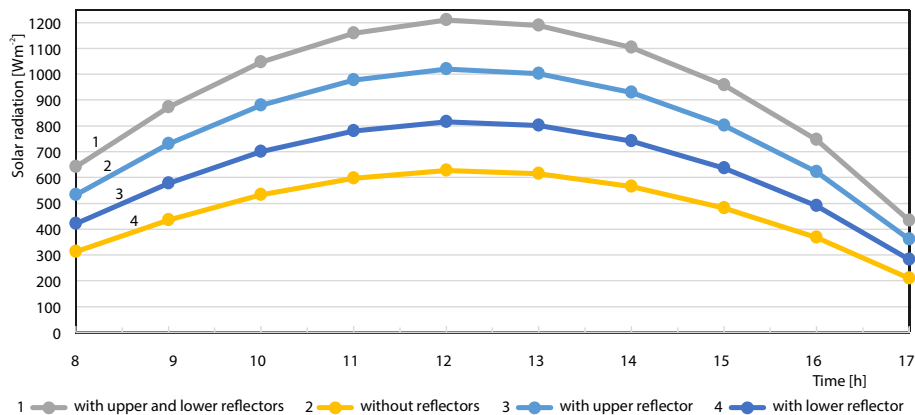


Figure 3. Variation of solar radiation with reflectors and without reflectors

The maximum value was 1139 W/m<sup>2</sup>, approximately 51% of the system when using the upper and lower reflective mirrors on the same day. Meanwhile, the maximum value of the total absorbed solar radiation with the presence of the upper or lower reflector alone was 951 W/m<sup>2</sup>, and 747 W/m<sup>2</sup>, respectively. These results are consistent with the results of [11]. This amount of absorbed solar radiation was then used as an input variable for the performance calculations.

### Temperature of PV panel

Figure 4 shows the comparison between the PV panel temperatures for different operating conditions at 1% nanofluid mass fraction. The results showed that the panel surface temperature produced the same behavior of the absorbed solar radiation. The temperature of solar cell surface increased in the first hours of testing till midday and then decreased as the intensity of solar radiation decreased till sunset [8, 12]. The highest temperature of the cell surface using the nanofluid and two reflectors together was 63.67 °C whereas the conventional PV/T collector (with nanofluid and without reflectors) was 44.3 °C at midday, which means that thermal performance increased in the case of using the reflectors and nanofluid. The existence of reflectors and nanofluid as a cooling material leads to the increasing in the rates of different temperatures in PV/T collector corresponding to the behavior of conventional solar collectors [5, 10].

### Temperature of outlet water

Figure 5 displays the comparison of the water outlet temperature for the eight model previously discussed. It was noticed that the outlet water temperatures were increasing throughout the period between 9 a. m. and 1 p. m., which indicates that the useful energy,  $\bar{Q}_{us}$  was higher than that carried out by the load water. After 1 p. m., these temperatures started decreasing because the value of useful energy became lower than the energy carried out by the load water. The outlet temperature reached the maximum value of (50.021 °C) for the system (two reflec-

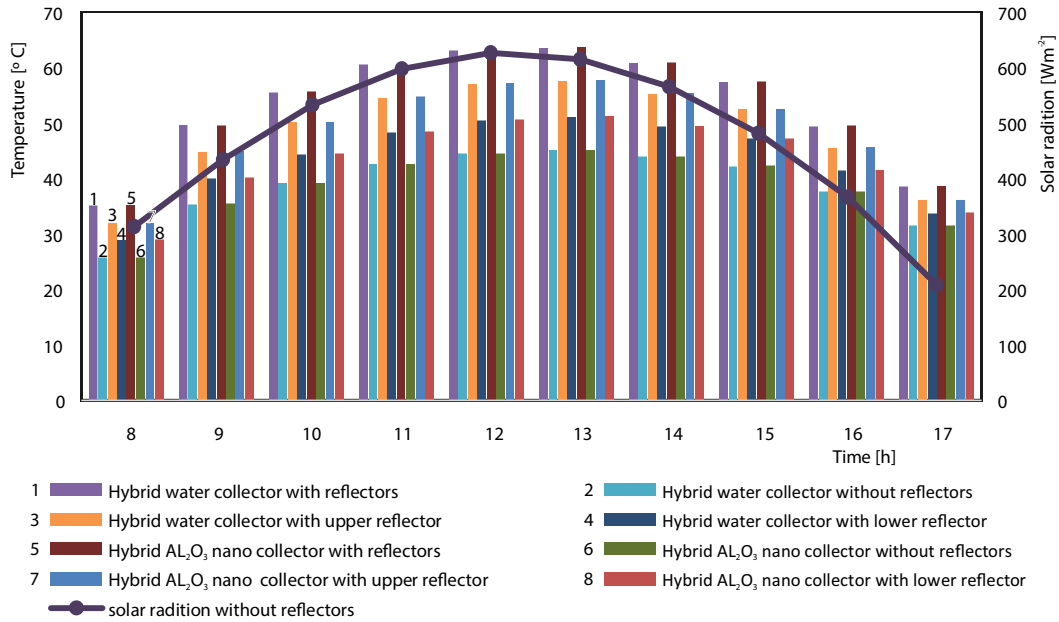


Figure 4. Variation of solar cell temperature for different operating conditions

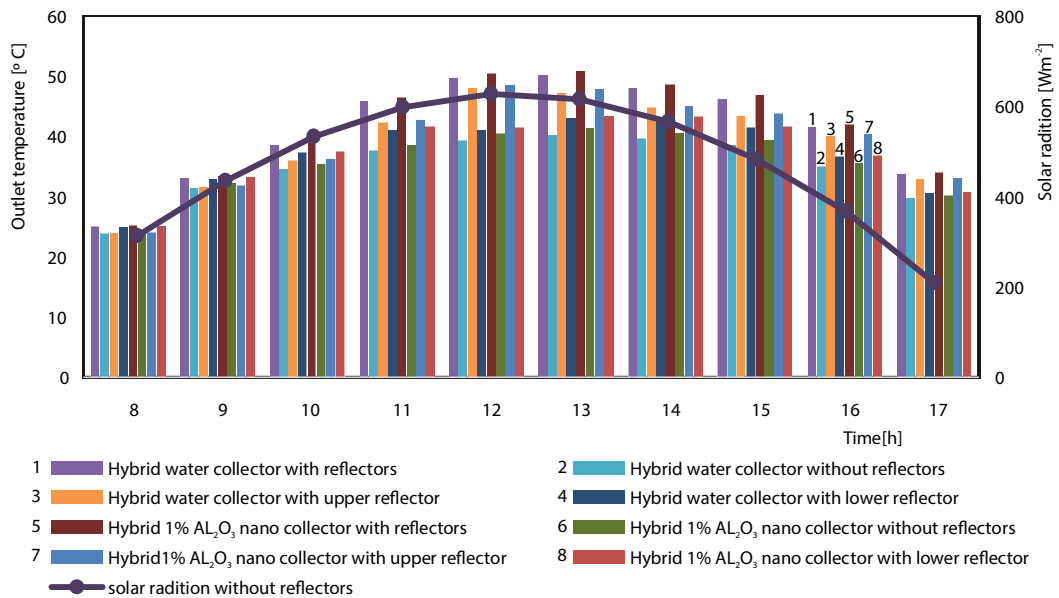
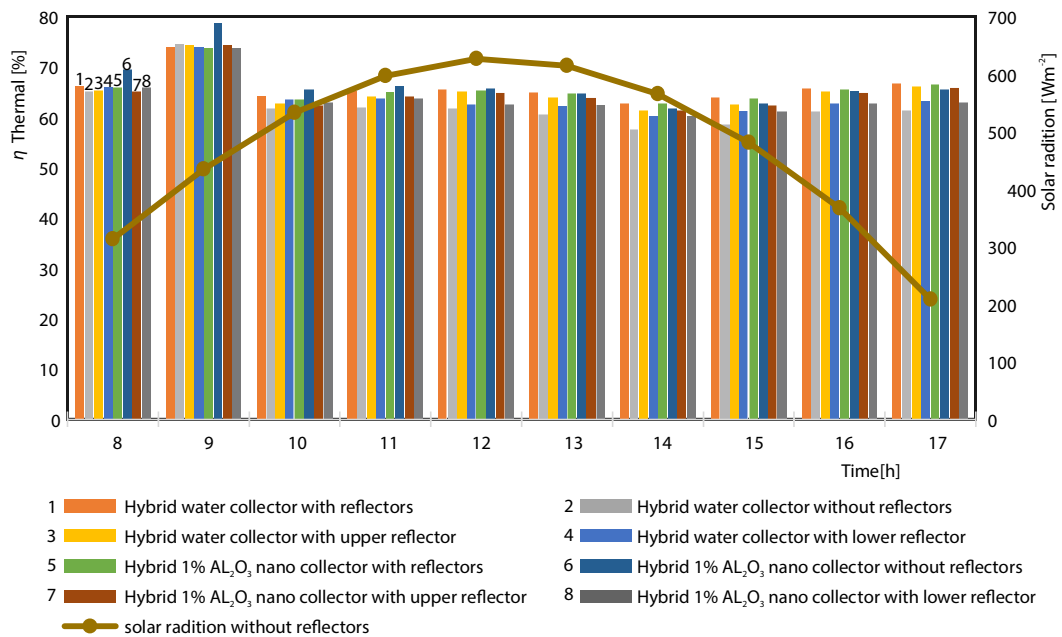


Figure 5. Variation of outlet water temperature for different operating condition

tors and 1% nanofluid mass fraction), whereas in the case of the conventional PV/T collector (without nanofluid and reflectors), the temperature was 39 °C at 1 p. m. The reason behind the rise in the temperature of the solar cell was the existence of the reflectors. These results accorded with the published literature [6, 15, 26].

*Thermal and electrical efficiencies*

The variation of useful transferred energy follows closely the variation of solar intensity. Figure 6 shows that there was a high increase in the thermal efficiency during the first hours of the operating period 8-10 a. m. for all cases. This is because of the large increase in the net energy absorbed due to the presence of mirrors, coupled with relatively small heat losses from the collector to the ambient atmosphere because of the low temperature of the cell surface which reduces the thermal losses. The instantaneous efficiency also reached its maximum value of 66.57 % at 9 a. m. for the hybrid collector without a reflector and then decreased. This trend is due to the increasing heat losses with the time of the day accompanied with decreasing net energy absorbed in the afternoon hours. The time at which the maximum instantaneous efficiency occurrence was found to be different for dissimilar conditions. It was also observed that on the second half of the day (after 2 p. m.), there was a noticeable increase in the instantaneous efficiency resulting from an increase in the useful energy transferred. The hybrid collector with two reflectors and without using the nanofluid was found to be more efficient than other systems. It was also noticed that the using of nanofluid reduced the daily thermal efficiency for different cases [38].



**Figure 6. Variation of thermal efficiency,  $\eta_{th}$ , with time for different cases (1% concentration)**

The existence of the reflective mirrors increased the thermal efficiency due to the rise of solar radiation that occurred on the surface of the solar cell. Hence, this choice is deemed favorable for getting the highest energy and also agreeable with the results of published articles [3]. The average of daily thermal efficiency as a result of using two reflectors without nanofluid was 62.1% ,while the thermal efficiency without using any reflector was 59.735%. This indicates a positive effect of using reflectors on the thermal efficiency [8]. Figure 7 shows the electrical efficiency following the solar radiation except near noon because the increase of the solar panel temperature caused the decrease in the electrical efficiency for all cases. It was

observed from the figure that the system using the  $\text{Al}_2\text{O}_3$ -water cooling without reflectors had the highest efficiency with the maximum value of daily electrical efficiency was 14.6%. It can be seen that the electrical efficiency was reduced with the existence of the reflective mirrors, whereas the daily average of the total electrical efficiency without the reflective mirror and using the nanofluid was 14.6%, while with a reflective mirror and using nanofluid, the daily average was 13.67%. This is related to the reflective mirror which increases the solar radiation that leads to the increase of the solar cell temperature and means a reduction in its efficiency. It was also noticed that the increase in electrical efficiency in the first morning hours was due to the decrease in the temperature of solar cell, then started to decline gradually at noon due to the increase in the temperature of the solar cell and after that started to rise slightly in the afternoon, and then began to reduce due to the decline the solar radiation quantity reaching the solar cell. This agreed with the experimental results from the previous studies [12, 39]. It was also noted that the total efficiency values of most of the designs were semi-equal. It was also noted that the overall efficiency increased in the presence of the reflective mirror and decreased with the used of  $\text{Al}_2\text{O}_3$ -water as a cooling media [40].

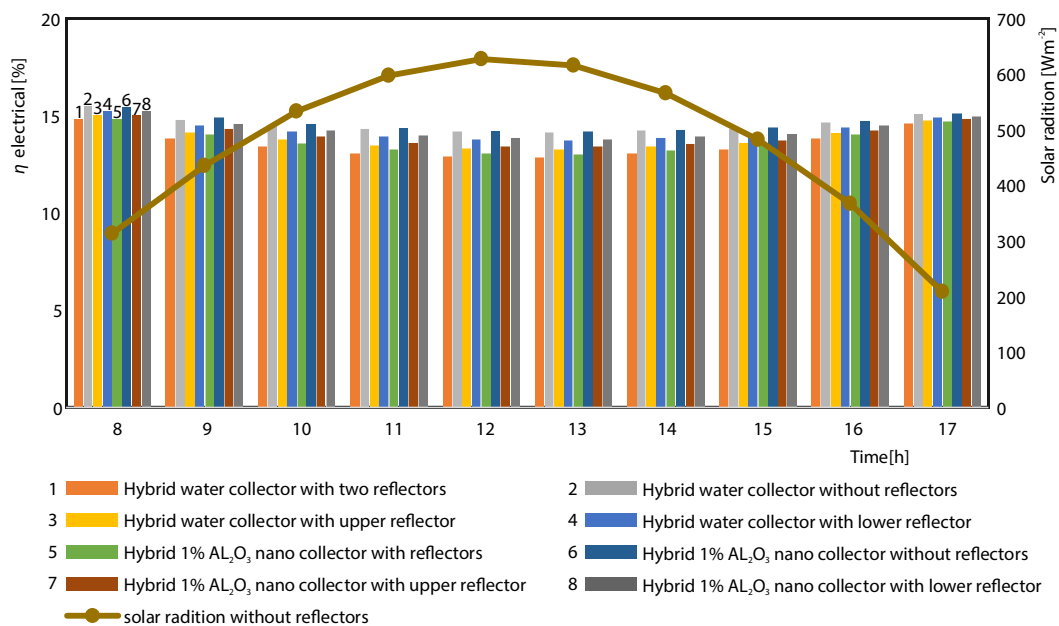


Figure 7. Variation of electrical efficiency with time for different cases (1% concentration)

## Conclusions

In the present article, the common effect of reflective mirror and nanofluid on the performance of a PV/T water collector was discovered. From the finding of the previous sections, the following results are obtained.

- The existence of reflectors and nanofluid as cooling materials leads to the increase in the rates of different temperatures in PV/T collector corresponding to the behavior of conventional solar collectors.
- The outlet water temperature increased by 21.7%, while the outlet water temperature increased by 0.44% when nanofluid was used as a cooling medium.

- The usage of reflective mirrors was the main factor in the enhancement of the performance of the PV/T collector compared to the use of nanofluid.
- The system using the Al<sub>2</sub>O<sub>3</sub>-water cooling without reflectors had the highest electrical efficiency; the maximum value of daily electrical efficiency was 14.6%. It was also noticed that the using of nanofluid reduced the daily thermal efficiency for different cases.

### Nomenclatures

$A_c$	– collector surface area, [m <sup>2</sup> ]
$B$	– coefficient of PV cell, ( $\beta=0.0045\text{ }^\circ\text{C}^{-1}$ ) temperature coefficient of efficiency, [–]
$c_n$	– heat capacity of the nanomaterial (Al <sub>2</sub> O <sub>3</sub> ), [Jkg <sup>-1</sup> °C <sup>-1</sup> ]
$c_w$	– heat capacity of the base fluid (water), [Jkg <sup>-1</sup> °C <sup>-1</sup> ]
$C_{\text{eff}}$	– heat capacity of nanofluid, [Jkg <sup>-1</sup> °C <sup>-1</sup> ]
$I_{\text{total}}$	– total absorbed radiation on the collector surface, [Wm <sup>-2</sup> ]
$I_b$	– beam radiation on the collector surface, [Wm <sup>-2</sup> ]
$I_d$	– diffuse solar radiation, [Wm <sup>-2</sup> ]
$I_{\text{up-ref}}$	– component of solar radiation reflected from upper reflector, [Wm <sup>-2</sup> ]
$I_{\text{lo-ref}}$	– component of solar radiation reflected from lower reflector, [Wm <sup>-2</sup> ]
$I_g$	– solar radiation reflected from the ground, [Wm <sup>-2</sup> ]
$I_{\text{diffuse}}$	– diffused radiation, [Wm <sup>-2</sup> ]
$K_{\text{eff}}$	– thermal conductivity of nanofluid, [Wm <sup>-1</sup> K <sup>-1</sup> ]
$K_w$	– thermal conductivity of water, [Wm <sup>-1</sup> K <sup>-1</sup> ]
$K_n$	– thermal conductivity of nanoparticle, [Wm <sup>-1</sup> K <sup>-1</sup> ]
$\dot{m}$	– mass-flow rate, [kgs <sup>-1</sup> ]
$m_n$	– mass of the nanomaterial
$m_w$	– mass of the base fluid
$P_{\text{refl}}$	– Prandtl number ( $=\mu_{\text{eff}}C_{\text{eff}}/K_{\text{eff}}$ ), [–]
$\dot{Q}_u$	– total thermal energy gain, [Wm <sup>-2</sup> ]

$S_{\text{total}}$	– total absorbed solar radiation, [Wm <sup>-2</sup> ]
$T_a$	– ambient air temperature, [°C]
$T_{\text{PV},m}$	– solar cell temperature, [°C]
$T_{f,\text{in}}$	– air temperature at the inlet, [°C]
$T_{f,\text{out}}$	– air temperature at the outlet, [°C]
$T_o$	– temperature of solar cell at standard condition, ( $T_o = 25\text{ }^\circ\text{C}$ )

### Greek symbols

$\alpha$	– solar altitude angle, [°]
$\alpha_{\text{PV}}$	– thermal absorbance of cell, [–]
$\alpha_1$	– angle between upper reflector and horizontal plane, [°]
$\alpha_2$	– angle between lower reflector and vertical plane, [°]
$\beta$	– collector tilted plane angle, [°]
$\delta$	– declination angle of the Sun, [°]
$\eta_{\text{ele}}$	– electrical efficiency, [–]
$\eta_{\text{PV}}$	– instantaneous electrical efficiency, [–]
$\eta_{\text{th}}$	– thermal efficiency, [–]
$\mu_{\text{eff}}$	– nanofluid viscosity, [kgm <sup>-1</sup> °C <sup>-1</sup> ]
$\mu_w$	– water viscosity, [kgm <sup>-1</sup> °C <sup>-1</sup> ]
$\rho_{A1}$	– reflectance from mirrors, [–]
$\rho_g$	– ground reflectance, [–]
$\rho_{\text{eff}}$	– density of the nanofluid, [kgm <sup>-3</sup> ]
$\rho_n$	– density of the nanoparticle, [kgm <sup>-3</sup> ]
$\rho_w$	– density of the water, [kgm <sup>-3</sup> ]
$\tau\alpha$	– transmittance-absorbance product, [–]
$\phi$	– volume concentration of the nanoparticles

### References

- [1] Ahmed, O. K., *et al.*, Influence of Porous Media on the Performance of Hybrid PV/Thermal Collector, *Renewable Energy*, 112 (2017), Nov., pp. 378-387
- [2] Ahmed, O. K., *et al.*, Dust Effect on the Performance of the Hybrid PV/Thermal Collector, *Thermal Science and Engineering Progress*, 3 (2017), Sept., pp. 114-122
- [3] Kostić, L. T., *et al.*, Optimal Design of Orientation of PV/T Collector with Reflectors, *Applied Energy*, 87 (2010), 10, pp. 3023-3029
- [4] Kostić, L. T., *et al.*, Influence of Reflectance from Flat Aluminum Concentrators on Energy Efficiency of PV/Thermal Collector, *Applied Energy*, 87 (2010), 2, pp. 410-416
- [5] Tabet, I., *et al.*, Performances Improvement of Photovoltaic Thermal Air Collector by Planer Reflector, *Rev. des Energies Renouvelables*, 1 (2014), pp. 219-225
- [6] Naik, P. S., Palatel, A., Energy and Exergy Analysis of a Plane Reflector Integrated Photovoltaic – Thermal Water Heating System, *ISRN Renewable Energy*, 2014 (2014), ID180618
- [7] Baccoli, R., *et al.*, A Mathematical Model of a Solar Collector Augmented by a Flat Plate above Reflector: Optimum Inclination of Collector and Reflector, *Energy Procedia*, 81 (2015), Dec., pp. 205-214
- [8] Bahaidarah, H. M., *et al.*, A Combined Optical, Thermal and Electrical Performance Study of a V-trough PV System-Experimental and Analytical Investigations, *Energies*, 8 (2015), 4, pp. 2803-2827

- [9] Belhadj, M., Modeling of Automatic Reflectors for PV Panel Attached to Commercial PV/T Module Modeling of Automatic Reflectors for PV panel Attached to Commercial, *International Journal of Applied Engineering Research.*, 11 (2016), 23, pp. 11309-11314
- [10] Chowdhury, N., Design and Experimental Validation of a Photovoltaic-Thermal (PVT) Hybrid Collector, *International Journal of Renewable Energy Research*, 6 (2016), 4, pp. 1446-1453
- [11] Rosli, M. A., *et al.*, Thermal Performance on Unglazed Photovoltaic Thermal Polymer Collector, *Advanced Materials Research*, 911 (2014), Mar., pp. 238-242
- [12] Soltani, S., *et al.*, An Experimental Investigation of a Hybrid Photovoltaic/Thermoelectric System with Nanofluid Application, *Solar Energy*, 155 (2017), Oct., pp. 1033-1043
- [13] Mustafa, W., *et al.*, Numerical Investigation for Performance Study of Photovoltaic Thermal Nanofluid System, *Proceedings, Science and Engineering Technology International Conference*, Langkawi, Malaysia, 2017
- [14] Colangelo, G., *et al.*, Performance Evaluation of a New Type of Combined Photovoltaic – Thermal Solar Collector, *Journal of Solar Energy Engineering*, 137 (2015), 4, pp. 1-12
- [15] Tripathi, R., *et al.*, Energy Matrices Evaluation and Exergoeconomic Analysis of Series Connected N Partially Covered (Glass to Glass PV Module) Concentrated-Photovoltaic Thermal Collector: At Constant Flow Rate Mode, *Energy Conversion and Management*, 145 (2017), Aug., pp. 353-370
- [16] Hussein, H. A., *et al.*, Improving the Hybrid Photovoltaic/Thermal System Performance Using Water Cooling Technique and (Zn-H<sub>2</sub>O) nanofluid, *International Journal of Photoenergy*, 2017 (2017), ID6919054
- [17] Ghadiri, M., *et al.*, Experimental Investigation of a PVT System Performance using Nano Ferrofluids, *Energy Conversions and Management*, 103 (2015), Oct., pp. 468-476
- [18] Kim, J. H., *et al.*, Comparison of Electrical and Thermal Performances of Glazed and Unglazed PVT Collectors, *International Journal of Photoenergy*, 2012 (2012), ID957847
- [19] Al-Shamani, A., *et al.*, Experimental Studies of Rectangular Tube Absorber Photovoltaic Thermal Collector with Various Types of Nanofluids under the Tropical Climate Conditions, *Energy Conversions and Management*, 124 (2016), Sept., pp. 528-542
- [20] Sardarabadi, M., *et al.*, Experimental Investigation of the Effects of Using Metal-oxides/water nanofluids on a Photovoltaic Thermal System (PVT) from Energy and Exergy Viewpoints, *Energy*, 138 (2012), Nov., pp. 682-695
- [21] Potenza, M., *et al.*, Experimental Investigation of Transparent Parabolic trough Collector Based on Gas-phase Nanofluid, *Applied Energy*, 203 (2017), Oct., pp. 560-570
- [22] Colangelo, G., *et al.*, Numerical Simulation of Thermal Efficiency of an Inovative Al<sub>2</sub>O<sub>3</sub> Nanofluid Solar Thermal Collector, *Influence of Nanoparticles Concentration*, 21 (2017), 6, pp. 2769-2779
- [23] Chemisana, D., *et al.*, Experimental Performance of a Fresnel-Transmission PVT Concentrator for Building-Façade Integration, *Renewable Energy*, 85 (2016), Jan., pp. 564-572
- [24] Duffie, J. A., *et al.*, *Solar Engineering of Thermal Processes*, John Wiley and Sons Inc., New York, USA, 2013
- [25] Ahmed, O. K., *et al.*, *Principle of Renewable Energies*, Foundation of Technical Education, Baghdad, Iraq, 2011
- [26] Maadi, S. R., *et al.*, Characterization of PVT Systems Equipped with Nanofluids-Based Collector from Entropy Generation, *Energy Conversions and Management*, 150 (2017), Oct., pp. 515-531
- [27] Milanese, M., *et al.*, An Investigation of Layering Phenomenon at the Liquid – Solid Interface in Cu and CuO Based Nanofluids, *International Journal of Heat and Mass Transfer*, 103 (2016), Dec., pp. 564-571
- [28] Colangelo, G., *et al.*, Cooling of Electronic Devices: Nanofluids Contribution, *Applied Thermal Engineering*, 127 (2017), Dec., pp. 421-435
- [29] Ahmed, O.K., Experimental and Numerical Investigation of Cylindrical Storage Collector (Case Study), *Case Studied in Thermal Engineering*, 10 (2017), Sept., pp. 362-369
- [30] Allan, J., The Development and Characterisation of Enhanced Hybrid Solar Photovoltaic Thermal Systems, Ph. D. thesis, Brunel University, London, UK, 2015
- [31] Yazdanifard, F., *et al.*, Performance of Nanofluid-Based Photovoltaic/Thermal Systems: A Review, *Renewable and Sustainable Energy Reviews*, 76 (2017), Sept., pp. 323-352
- [32] Ahmed, O. K., *et al.*, Effect of the Shape Surface of Absorber Plate on Performance of Built-in-Storage Solar Water Heater, *Journal of Energy and Natural Resources*, 3 (2014), 5, pp. 58-65
- [33] Ahmed, O. K., *et al.*, Theoretical and Experimental Study of the Effect of Design and Operational Variables on the Performance of Hybrid Solar Air Heater, *Proceedings, 2<sup>nd</sup> Scientific International Conference*, Erbil, Iraq, 2017, pp. 1-7

- [34] Amori, K. E., *et al.*, Field Study of Various Air Based Photovoltaic/Thermal Hybrid Solar Collectors, *Renewable Energy*, 63 (2014), Mar., pp. 402-414
- [35] Florschuetz, L. W., Extension of the Hottel-Whillier Model to the Analysis of Combined Photovoltaic/Thermal Flat Plate Collectors, *Solar Energy*, 22 (1979), 4, pp. 361-366
- [36] Manokar, A. M., *et al.*, Performance Analysis of Parabolic trough Concentrating Photovoltaic Thermal System, *Procedia Technology*, 24 (2016), Dec., pp. 485-491
- [37] Othman, M. Y., *et al.*, Performance Analysis of PV/T Combi with Water and Air Heating System: An Experimental Study, *Renewable Energy*, 86 (2016), Feb., pp. 716-722
- [38] Visconti, P., *et al.*, Measurement and Control System for Thermo-Solar Plant and Performance Comparison between Traditional and Nanofluid Solar Thermal Collector, *International Journal on Smart Sensing and Intelligent System*, 9 (2016), 3, pp. 1220-1242
- [39] Kessentini, H., *et al.*, Numerical and Experimental Study of an Integrated Solar Collector with CPC Reflectors, *Renewable Energy*, 57 (2013), Sept., pp. 577-586
- [40] Iacobazzi, F., *et al.*, An Explanation of the  $\text{Al}_2\text{O}_3$  Nanofluid Thermal Conductivity Based on the Phonon Theory of Liquid, *Energy*, 116 (2016), Part 1, pp. 786-794